American Journal of Engineering Research (AJER)
e-ISSN: 2320-0847 p-ISSN : 2320-0936
Volume-5, Issue-12, pp-21-31
www.ajer.org
Research Paper Open Access

Identification of Volcano Hotspots in Multi Spectral ASTER Satellite Images usingDTCWT Image Fusion and ANFIS Classifier

Mr. S. Muni Rathnam[1], Dr. T. Ramashri,
[1]*Research Scholar, Dept. ofECE, SVU College Of Engg., SVU Tirupati, Andhra Pradesh, India.*
[2]*Professor, Dept. ofECE, SVU College Of Engg., SVU Tirupati, Andhra Pradesh, India.*

ABSTRACT: Volcanic hotspots identification and monitoring can play crucial role in planning and extraction of disaster management. Satellite images have become able alive in this crucial domain to help in the identification of volcano hotspots. This research work aims to implement an automated volcanic hotspots detection approach using Adaptive Neuro Fuzzy Inference System (ANFIS)classifier. In order to improve classification accuracy and performance, a Dual Tree Complex Wavelet Transform (DTCWT) has been employed to fuse the volcano images in different spectrums visible and visible near infrared. The fused images subsequently used for extraction of features with help of Discrete Wavelet Transform (DWT) and Principle Component Analysis (PCA). ANFIS classifier takes these features as input and delivers classification in the way of indicating the possible absence and presence of volcano in that particular image. The approach is validated with help of ASTER volcanic data base, the classifier performance has been evaluated for computing different performance measures. The results demonstrate the improved accuracy that can be brought out by using fused images in the identification of volcano hotspots.
Keywords: Volcano, Satellite images, ANFIS, DTCWT, DWT, PCA and ASTER

I. INTRODUCTION

Earth's lithosphere (i.e upper most solide mantle) is broken into a seven series of slabs called "Tectonic plates". These plates are rigid and move with constant velocity on hard & soft layers in the interior of the earth. The plates may move upward, downward or side. If the plates move towards then it is called "Convergent plates" and if recede then it is known as "Divergent plates". The movement of plates creates gaps between them in which pressure builds up that yields very high temperature. Due to high temperature rocks, metals etc., melt and forms magma this is called "Volcano". Magma rising from lower reaches and gathers in a reservoir in the weak portion of the overlying rock is called magma chamber. When magma reaches the surface of earth is called "Lava" and the main composition of lava is silica and amount of silica determines the level of viscosity. Volcanoes in the islands form due to movements between two oceanic plates and others volcanoes forms between oceanic &continental plates. Other reason to form volcanoes is plumes, It is bubble of materials which rises to the surface layers from the deep interior of the earth. The plumes are form when the deep mantle is heated to several hundred degrees hotter than its surroundings. The plume portion becomes lighter than surroundings forms like hot air balloon and plume may take mushroom shape. The plume may move upward direction and opens the surface of the earth which results volcano eruption.

Among the natural hazards, Volcano is one of the most dangerous because it effects both environment and living things. The causes of volcanoes are Tsunamis & Earthquakes, Damage to Public & Private Properties, Landslides, Ground deformation, Transport and communication will be blocked, Volcanic ash can be a threat to Aircraft, Ash can cause breathing problems, Loss of lives, Loss of crops, Lahars, Acid rain, Hole in ozone layer, Carbon dioxide trapped in low lying areas can lethal to people and animals, Unpleasant smells, Volcanic gases are harmful to health, infrastructure and vegetation.

The explosive growth of remote sensing technology, internet and multimedia systems poses great challenge in handling huge amount of data. Advancement in the field of Remote Sensing has gone to an extent of taking the geospatial accuracy to few centimeters. Currently remote sensing has become a tool in the hands of scientific community to develop modeling applied in the projection right from natural disasters. With the rapid development in remote sensing, digital image processing becomes an important tool for quantitative andstatistical interpretation of remotely sensed images.

The use of remote sensing within the domain of natural hazards and disasters has become increasingly common, to increase awareness of environmental issues such as climate change, but also to the increase in geospatial technologies and the ability to provide up-to-date imagery to the public through the media and internet. One of the advantages of remote sensing is that the measurements can be performed from a great distance (several hundred or even several thousand kilometers in the case of satellite sensors), which means that large areas on ground can be covered easily. With satellite instruments it is also possible to observe, a target repeatedly; in some cases every day or even several times per day.

Nowadays, satellite imaging is one of the most important sources of geographical, geophysical and environmental information. Satellite images are important source of information which is used in many environmental assessments and monitoring of agriculture, meteorology etc. They are important available data sources for map generation and updating of available maps. They provide accurate easily accessible and reliable spatial information for Geographical Information Systems. The advanced technology where most satellite images are recorded in digital format virtually, all image interpretation and analysis involve some elements of digital processing. Increasing use of satellite images which are remotely sensed images acquired periodically by satellites on different areas and for multiple purposes makes it extremely interesting for various applications.

Education and knowledge are important keys for human being. The correlation between education and the prosperity of society is well established. The importance of education has been universally acknowledged and accepted, but the phenomenon of exclusion of larger sections of the population and the drop outs from the formal education systems is one constraint. Academic and professional up-gradation, the professional training that would enhance the performance in traditional occupations and the intellectual growth, is required in today's time. Image fusion is the procedure of merging information from a corresponding set of images into one image, wherein the resultant fused image may be informative. Image fusion is done at pixel, feature and decision processing levels.

II. REVIEW OF LITERATURE

Sweta K. Shah et al.[1] have compared the performance of image fusion technique in Spatial domain Principal Component Analysis (PCA) and Transform domain Discrete Wavelet Transform is Frequency domain technique with respect to spatial frequency and Standard deviation, Concluded that the performance of DWT image fusion is better than the Spatial domain PCA technique. T. Ramashri et al.[2] have studied the different wavelet transform image fusion techniques such as symlet, bio-oethogonal, meyer&reverse bio-orthogonal wavelets and Compared the performance using mean, Standard Deviation, Entropy, Correlation Coefficient, Covariance RMS Error & PSNR.

Asha Das et al.[3]applied wavelet based multi resolution pyramid image fusion technique to remote sensed satellite images of low spatial resolution multispectral & high resolution panchromatic images. Segmentation is performed on the fused images and compared with conventional fusion methods. Vaibhav R. Pandit et al [4] have reviewed the image fusion for remote sensing applications. Panchromatic and hyper spectral images are fused to increase the both spatial and spectral resolutions. PCA, Gram-Schmidt, Wavelet Transform, Curvelet Transform and ContourletTransform image fusion techniques are compared using thirteen performance evaluation parameters.Tasneem Ahmed et al.[5] used Genetic algorithm image fusion technique to fuse MODIS and PALSAR-1 data and contextual threshold technique for detecting hotspot. The quality of fused image is measured by suing RMS error, PSNR, RMD and UQI.Hyung-Sup Jung et al. [6] have discussed the multi sensor fusion of landsat8 thermal infrared and panchromatic image. This technique improved the object recognition of the TIR image while preserving spatial details of the PAN image and the thermal information of object to the PAN image while maintaining the thermal information of the TIR image. This fusion technique is effectively applied to detect the volcanic activity, radiative exposure of nuclear power plant and surface temperature change with respect to land use change. Masthanaiahet. Al [7] have developed image fusion technique by integrating PCA, Wavelet &CurveletTransform for MRI, CT, Multi-spectral and panchromatic images and performance is compared using performance evaluation parameters.

OguzGungor et al. [13] explained principles, implementation and evaluation of wavelet transform based image fusion. 2D discrete wavelet transform is used, the wavelet coefficients for fused image are taken based on maximum magnitude criteria. The performance is compared with PCA, Brovey and Multiplicative transform approaches. ShutaoLi[14] presented stationary wavelet transform image fusion for remote sensed images and Spectral discrepancy & Spatial distortion are used to measure the quality of the image fusion.

Alessandro Piscini et al. [15] have discussed the classification of volcano hospots using Artificial Neural Networks with back propagation training. AVHRR satellite dataset is used for raining and testing the ANN. The training is done by extracting thermal features from both hotspot and normal satellite images. The cent present classification accuracy is obtained for cloud free images and accuracy decreased in the case of cloud cover images. The classifier is able to classify only Etna volcano because it is trained with Etna volcano images.

III. METHODOLOGY

Proposed Algorithm

Step1: Create training & testing dataset using ASTER Satellite image gallery.
Step2: Find the 3 level decomposition of training images using Daubechies (db_4) wavelet.
Step3: Find Principle Component Analysis (PCA) for Decomposed images.
Step4: Extract the statistical parameters.
Step5: Train the ANFIS classifier using extracted statistical Parameters.
Step6: Plot mean square error.
Step7: Fuse visible and VNIR images in test data set using Dual Tree Complex Wavelet Transform (DTCWT).
Step8: Test the trained ANFIS using fused test set.
Step9: Calculate performance evaluation parameters.

Data Set

The training & testing data set is created using Advanced Space borne Thermal Emission and Reflection Radiometer (ASTER) image gallery[23]. The ASTER is one of the five state of art instrument sensor system on board terra with a unique combination of wide spectral coverage and high special resolution in the visible and near infrared through short wave infrared to the thermal infrared region. ASTER is a partnership between NASA, Japan's Ministry of Economy Trade and Industry (METI), National Institute of Advanced Industrial Science and Technology (AIST) and Japans Space Systems. ASTER data contributes to a wide array of global change related application areas including vegetation, ecosystem dynamics, hazard monitoring, geology, soil, hydrology and land cover change. Special features of ASTER are

- The Visible and Near Infra-Red (VNIR) telescope's backward viewing band for high resolution.
- Multispectral thermal infrared data of high spatial resolution.
- Highest spatial resolution surface spectral reflectance, temperature and emissivity data within the terra instrument suite.
- Capability to schedule on-demand data acquisition requests. Swath width is 60 Km.
- Orbital height is 705 Km from the ground.
- Temporal resolution is one day.

ASTER consists of three different sub systems

- Visible and Near Infra-Red (VNIR) has three bands with a spatial resolution of 15m
- Short Wave Infra-Red (SWIR) has 6 bands with a spatial resolution of 30m.
- Thermal Infra-Red (TIR) has 5 bands with a spatial resolution of 90m.
  Spatial, Spectral and Radiometric resolutions are shown in the table 1

S.No	Sub System	Band no.	Spectral resolution(μm)	Spatial resol. (m)	Radiometric resol.(bits)
1.	VNIR	1	(0.52-0.60)	15	8
		2	(0.63-0.69)		
		3N	(0.78-0.86)		
		3B	(0.78-0.86)		
2.	SWIR	4	(1.6-1.7)	30	12
		5	(2.145-2.225)		
		6	(2.185-2.225)		
		7	(2.235-2.285)		
		8	(2.295-2.365)		
		9	(2.360-2.430)		
3.	TIR	10	(8.125-8.475)	90	12
		11	(8.475-8.825)		
		12	(8.925-9.275)		
		13	(10.25-10.95)		
		14	(10.95-11.65)		

Table 1 : Spatial, Spectral and Radiometric Resolutions

In order to have the improved classifier accuracy, heterogeneous data set mix has been considered to train the proposed ANFIS classifier. The data set comprises of different images having the presence & absence of volcano in then. An image of different sizes, different resolutions & different bands has been considered in designing this data set. The purpose is to have a wide sense of categorization through data set mix that is

representative of different scenarios. Some of these scenarios includes considering images having different cloud covers, images captured at different altitudes and images having mix of sea and lands.

Discrete Wavelet Transforms

The avantage of wavelet transforms over Fourier transform is that, it has temporal resolution i.e it captures both frequency and location information [10]. A discrete wavelet transform (DWT) is any wavelet transform for which the wavelets are discretely sampled. Thus discrete wavelet transform (DWT) is a linear transformation that operates on a data vector whose length is an integer power of two, transforming it into a numerically different vector of the same length. It is a tool that separates data into different frequency components, and then studies each component with resolution matched to its scale. DWT is computed with a cascade of filters followed by a factor 2 sub sampling. The advantages of DWT are more robust, maintains good image quality and good spatial resolution at each level of decomposition. DWT transforms array of original sample into wavelet coefficients and IDWT Transforms wavelet coefficients into the original sampled data.

The Daubechies wavelet transform is named after inventing the mathematician Ingrid Daubechies. The db_4 transform has four wavelet and scaling functions coefficients.

The scaling function coefficients are $h_0 = \frac{1+\sqrt{3}}{4\sqrt{2}}$, $h_1 = \frac{3+\sqrt{3}}{4\sqrt{2}}$, $h_2 = \frac{3-\sqrt{3}}{4\sqrt{2}}$ and $h_3 = \frac{1-\sqrt{3}}{4\sqrt{2}}$ (1)

The wavelet function coefficients values are $g_0 = h_3$, $g_1 = -h_2$, $g_2 = h_1$ and $g_3 = -h_0$ (2)

The scaling and wavelet functions are calculated by taking the inner product of the coefficients and four data values as shown in below equations[11]

Scaling function: $a_i = h_0 s_{2i} + h_1 s_{2i+1} + h_2 s_{2i+2} + h_3 s_{2i+3}$ (3)

Wavelet function: $c_i = g_0 s_{2i} + g_1 s_{2i+1} + g_2 s_{2i+2} + g_3 s_{2i+3}$ (4)

H and *L* denote high and low-pass filters respectively followed by subsampling. Outputs of these filters are given by equations

$$a_{j+1}[p] = \sum_{n=-\infty}^{+\infty} l[n-2p]a_j[n] \quad (5)$$

$$c_{j+1}[p] = \sum_{n=-\infty}^{+\infty} h[n-2p]a_j[n] \quad (6)$$

Elements a_j are used for next step (scale) of the transform and elements c_j, called wavelet coefficients, determine output of the transform. *l[n]* and *h[n]* are coefficients of low and high-pas filters respectively as shown in figure1.

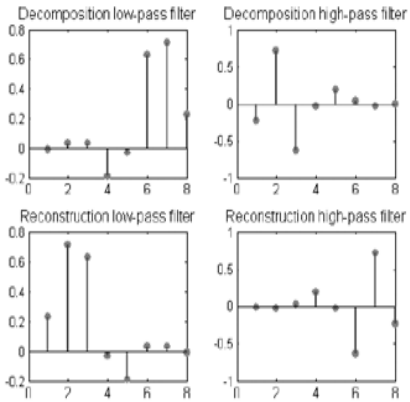

Figure1 : Filter coeffients

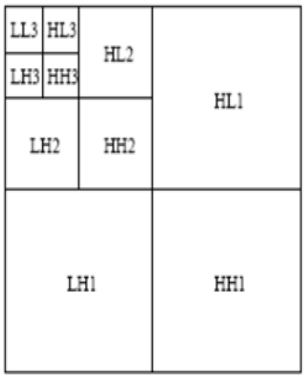

Figure2 : Three level decomposition

DWT involves decomposition of image into frequency channel of constant bandwidth. This causes the similarity of available decomposition at every level. DWT is implemented as multistage transformation. Level wise decomposition is done in multistage transformation. At level 1: Image is decomposed into four sub bands: LL, LH, HL, and HH where LL denotes the coarse level coefficient which is the low frequency part of the image. LH, HL, and HH denote the finest scale wavelet coefficient. The LL sub band can be decomposed further to obtain higher level of decomposition. This decomposition can continues until the desired level of decomposition is achieved for the application[9].

The LL subband is the result of low-pass filtering both the rows and columns and contains a rough description of the image. Therefore the LL subband is also called the approximation subband. The HH subband was high-pass filtered in both directions and contains the high-frequency components along the diagonals. The HL and LH images are the result of low-pass filtering in one direction and high-pass filtering in the other direction. LH contains mostly the vertical detail information, which corresponds to horizontal edges. HL

represents the horizontal detail information from the vertical edges. All three subbands HL, LH and HH are called the detail subbands, because they add the high-frequency detail to the approximation image. Three level decomposition is as shown in figure 2.

Principle Component Analysis (PCA)

PCA is also known as Karhunen-Loeve expansion, it is probably the most widespread multivariate statistical technique [8]. It is a method to study the structure of the data, with emphasis on determining the patterns of covariance among variables. Thus, PCA is the study of the structure of the variance-covariance matrix. In practical terms, PCA is a method to identify variable or sets of variables that are highly correlated with each other.As it removes the redundancy, it is used as data compression technique. PCA create an image subspace with reduced dimensionality, while maintaining a high level of discrimination between the images.

PCA method is also known as Eigenface Method, because reduced dimensionality is obtained using Eigen values and vectors.

Procedure:

Step1: Create 'M' training images with different size.
Step2: Construct Covariance matrix for individual images $C = AA^T$. Where A is image matrix in training set.
Step3: Find the Eigen values of the covariance matrix $|C-\lambda I| = 0$
Step4: Find Eigen vectors for Eigen values.
Step5: Form the Eigen vector matrix.
Step6: Calculate Statistical parameters of the above matrix.

Statistical Parameters

Let an intensity in Eigen value matrix 'Z' is assumed to be random variable whose value is varies from 0 to (L-1), where 'L' is no. of intensity levels is equal to 2^{N-1} and 'N' is no. of bits allocated to each pixel. The probability of random variable intensity 'Z' is called "Probability Density Function" (PDF) and denoted as$f_Z(z)$. In image processing, the probability density function is often called as "Histogram" and it is used to describe the nature of the image. The moment about origin or the first order statistical parameters can be obtained as follows

$$m_n = \sum_{i=0}^{L-1} {z_i}^n f_Z(z_i) \quad (7)$$

Where n = 1, 2, 3, 4 ……. is the order of the moments. m_1, m_2 are very useful parameters called mean & mean square in statistical analysis respectively. They called average or DC value & total power of an image respectively in electrical systems. The moments about mean or central moments can be obtained as follows

$$\mu_n = \sum_{i=0}^{L-1} (z_i - m_1)^n f_Z(z_i) \quad (8)$$

Where n = 1, 2, 3, 4 …….. is the order of central moments and m_1 is mean value. μ_1 is always zero, μ_2 is called variance in statistical analysis and ac power in electrical systems, Square root of μ_2 is called standard deviation in statistical analysis and rms value in electrical system if average value is zero, $\mu_3$and $\mu_4$are called skew and kurtosis respectively which describes the nature of probability density function or histogram.

The following nine parameters are extracted from the image for training & testing the ANFIS classifier.

Mean	$m_1 = \sum_{i=0}^{L-1} z_i f_Z(z_i)$	(9)
Mean square	$m_2 = \sum_{i=0}^{L-1} {z_i}^2 f_Z(z_i)$	(10)
Contrast	$\alpha_C = \sum_{i,j} \frac{x_{ij}}{1+\lvert i-j \rvert}$	(11)
Inverse Difference Movement	$\alpha_{IMD} = \sum_{i,j} \lvert i-j \rvert^2 x_{ij}$	(12)
Energy	$\alpha_E = \sum_{i,j} (x_{ij})^2$	(13)
Correlation	$\alpha_{CR} = \sum_{i,j} \frac{(i-m_{1i})(j-m_{1j})x_{ij}}{\sigma_i \sigma_j}$	(14)
Variance	$\mu_2 = \sum_{i=0}^{L-1} (z_i - m_1)^2 f_Z(z_i)$	(15)
Skew	$\mu_3 = \sum_{i=0}^{L-1} (z_i - m_1)^3 f_Z(z_i)$	(16)
Kurtosis	$\mu_4 = \sum_{i=0}^{L-1} (z_i - m_1)^4 f_Z(z_i)$	(17)

Where x_{ij} is the intensity value of the pixel at location (i,j), m_{1i}, m_{1j} are mean values and σ_i, σ_j are standard deviations with respect to i, j respectively.

ANFIS Classifier

The block diagram of proposed system is shown in figure 3, in which images from training set are wavelet decomposed at three levels, analyzed using PCA and then statistical features are extracted to train the ANFIS classifier.

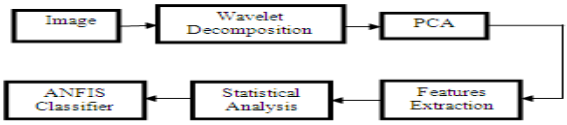

Figure 3. Block diagram of proposed system

The ANFIS combines both fuzzy logic principle and the concept of the neural networks. The ANFIS has advantage [16] of smoothness property fromthe fuzzy principle and adaptability property from the neural networks training structure. ANFIS contain five layers, membership function is generated in the first layer, and triangular membership function is used. Second layer multiplies incoming signals, weight normalization is done in the third layer, fuzzy rules generated in fourth layer and fifth layer acts as summer. The weights are adaptively changed based on rules generated errors. ANFIS training error plot and testing data set Vs ANFIS output are shown in figure 4 & 5 respectively.

The ANFIS combines both fuzzy logic principle and the concept of the neural networks. The ANFIS has advantages[12] such as smoothness property from the fuzzy principle and adaptability property from the neural networks training structure. Using advantageous of processing partial truth, it has been greatly utilized in engineering applications. The underlying network structure is a superset of all kinds of neural network paradigms with supervised learning capability. Neuro-fuzzy systems, is the combination of ANN with fuzzy systems, usually have the advantage of allowing an easy translation of the final system into a set of if-then rules, and the fuzzy system can be viewed as a neural network structure with knowledge distributed throughout connection strengths. Research and applications on neuro-fuzzy inference strategy made clear that neural and fuzzy hybrid systems are beneficial in fields such as the applicability of existing algorithms for artificial neural networks (ANNs), and direct adaptation of knowledge articulated as a set of fuzzy linguistic rules. An adaptive network, as its name implies, is a network structure consisting of nodes and directional links, overall input-output behavior is determined by the values of a collection of modifiable parameters through which the nodes are connected.

The adaptive system uses a hybrid learning algorithm to identify parameters of Sugeno-type fuzzy inference systems. It applies a combination of the least-squares method and the back-propagation gradient descent method for training FIS membership function parameters to emulate a given training data set.The network learns in two main phases. In the forward phase of the learning algorithm, consequent parameters identify the least squares estimate. In the backward phase, the error signals, which are the derivatives of the squared error with respect to each node output, propagate backward from the output layer to the input layer. In this backward pass, the premise parameters are updated by the gradient descent algorithm. Learning or training phase of the neural network is a process to determine parameter values to sufficiently fit the training data.

ANFIS training can use alternative algorithms to reduce the error of the training. A combination of the gradient descent algorithm and a least squares algorithm is used for an effective search for the optimal parameters. The main benefit of such a hybrid approach is that it converges much faster, since it reduces the search space dimensions of the back propagation method used in neural networks. A

NFIS are the fuzzy Sugeno model put in framework of the adaptive system which serves in model building and validation of developed model to facilitate training and adaptation. ANFIS training error plot and testing data set Vs ANFIS output are shown in figure 4 & 5 respectively.

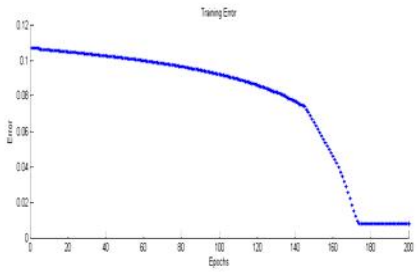

Figure 4 : Error plot in the training process

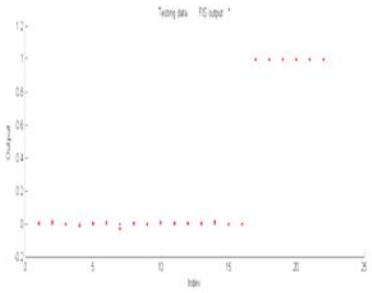

Figure 5 : Test data set Vs ANFISoutput

ANFIS Information

Number of nodes	: 78
Number of linear parameters	: 27
Number of nonlinear parameters	: 36
Total number of parameters	: 63

Dual Tree Complex Wavelet Transform

Fourier Transform approach for image fusion does not provide simultaneous localization in both space and frequency. Short Time FT is improved version of FT uses narrow windows so that non stationary appears to be stationary and it provides good spatial resolution but poor frequency resolution. DWT provides both spatial & frequency resolution but suffers with four fundamental problems [16].

- Wavelet coefficients oscillations around singularities as wavelets are band pass functions.
- Shift invariance: A small shift of the signal greatly distinguish the wavelet coefficient oscillation pattern around singularity.
- Aliasing is another problem, wavelet coefficients are computed via iterative discrete line decimations interspersed with non-ideal LP &HP resulting in substantial aliasing.
- Real wavelets are oriented along several directions due to which image features like ridges & edges becomes complicated[19].

Nick Kingsbury proposed two versions of 2D Dual Tree transform. The first one is Real Oriented 2D Dual Tree Transform withorientations in six distinct directions and approximate shift invariance. The second one is oriented 2D Dual Tree Complex WaveletTransform which is fully shifting invariant with orientations same as that of Real Oriented 2D Dual Tree Transform[21].

Let us consider 2D Wavelet $\Psi(x,y) = \Psi(x)\Psi(y)$ where $\Psi(x)\&\Psi(y)$ are row & column wise complex wavelet implementation and defined as[18]

$$\Psi(x) = \Psi_h(x) + j\ \Psi_g(x) \quad (18)$$

$$\Psi(y) = \Psi_h(y) + j\ \Psi_g(y) \quad (19)$$

$$\Psi(x,y) = \Psi_h(x)\Psi_h(y) - \Psi_g(x)\Psi_g(y) + j\,[\Psi_h(x)\Psi_g(y) + \Psi_g(x)\Psi_h(y)] \quad (20)$$

Real part of $\Psi(x,y) = \Psi_h(x)\Psi_h(y) - \Psi_g(x)\Psi_g(y)$ (21)

Imaginary part of $\Psi(x,y) = \Psi_h(x)\Psi_g(y) + \Psi_g(x)\Psi_h(y)]$ (22)

The plot of real, imaginary and magnitude of $\Psi(x,y)$ is as shown in the figure6, which shows the six directions $\pm15^o$, $\pm45^o$ and $\pm75^o$[17].

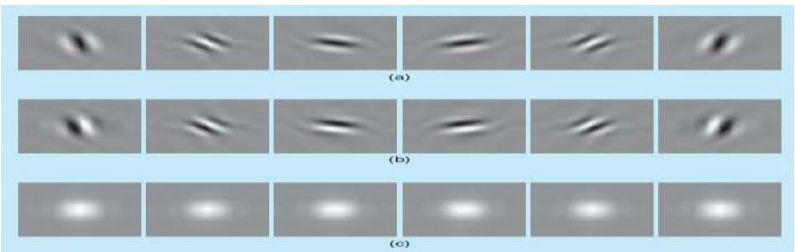

Figure6: Wavelets associated with the oriented 2D-dual tree CWT.(a)real part of complex wavelet (b)imaginary part and (c)illustrates the magnitude

The block diagram in figure7 explains how image decomposition can be achieved using 2D Dual Tree complex wavelet Transforms. The scaling functions $\Phi(x)$and $\Phi(y)$ are implemented using low pass filters and the wavelet functions $\psi(x)$ and $\psi(y)$ are implemented using high pass filters ,which forms Hilbert Transform Pairs[20].

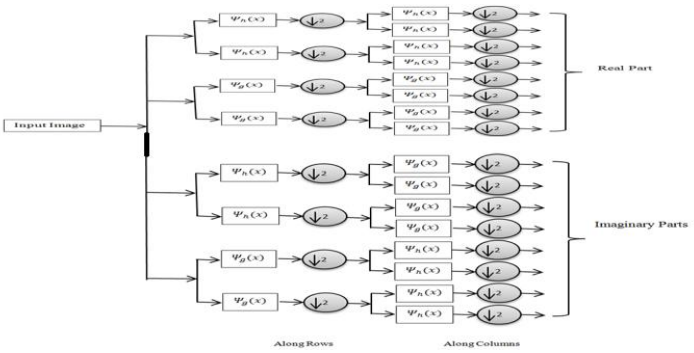

Figure 7: Image decomposition using DTCWT

To improve the classification accuracy, Visible range and Visible Near IR satellite volcano images [22] are fused using DT CWT as shown in figure8

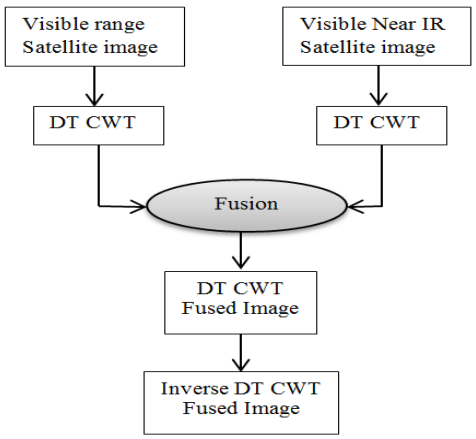

Figure8: Image fusion using DT CWT

IV. RESULTS AND DISCISSIONS

As a part of this work, GUI has been created with help of MATLAB which is shown in figure 9. The GUI helps in providing seamless interface in loading & analyzing the satellite images. The GUI has the scope to provide histogram analysis as well as color map function for better visualization of satellite images. DTCWT is used to fuse visible and visible near infrared images. The performance of the fusion image is evaluated by measuring mean, root mean square, and peak signal to noise ratio, correlation coefficient, covariance, entropy, spatial frequency and histogram plot.The histogram of visible , visible near infrared and fused volcano images are shown in figure 10, 11 & 12 respectively.

Figure 9: GUI for identifying volcano hotspots using fusion technique.

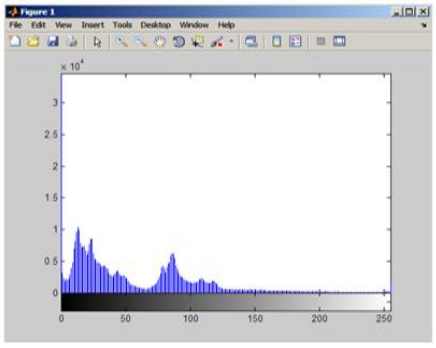

Figure 10 : Histogram of Visible range image

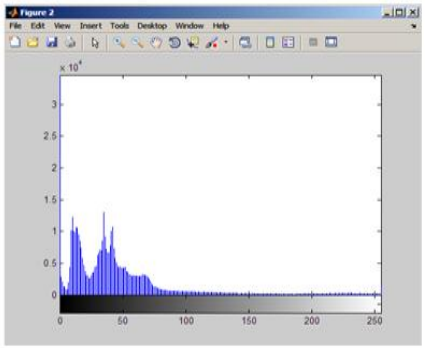

Figure 11 : Histogram of visible near infrared image

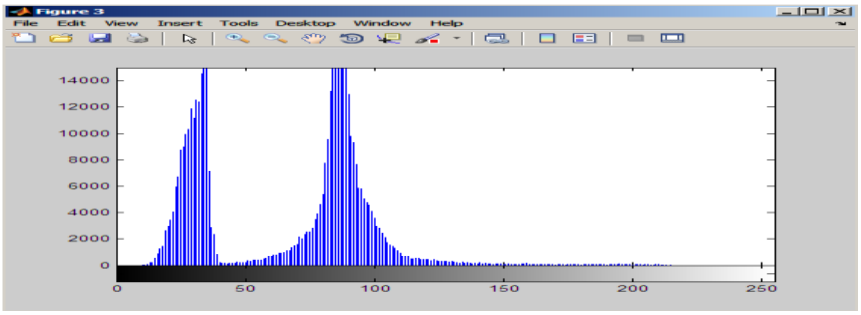

Figure 12 : Histogram of fused image

Different six test data sets are formed using ASTER data base by considering images of eight different volcanoes such as Etna, Barren Island, Mauna, Manam, Ulawun, Taal, Merapi and Nabro volcanoes.

Data Set1 contain 60 volcano imagesin visible range with zero percent cloud cover and 26 non volcano images. Data Set2 contain 157 volcano images in visible range with different percentage ofcloud covers and 26 non volcano Images Data Set3 contain 60 volcano images volcanoes invisible near infrared range with zero percent cloud cover and 26 non volcano images.Data Set4 contain 157 volcano images in visible near infrared range with different percent cloud cover and 26 non volcano images.Data Set5 is formed by fusing both visible & visible near infrared images of same volcano which are obtained at same time and same altitude. It contain fused 62 fused volcano images with zero percent cloud cover and 26 non volcano images.Data Set6 is formed by fusing both visible & visible near infrared images of same volcano taken at same time and same altitude with different percentages of cloud covers. It contain 157 fused volcano images and 26 non volcano images. The different performance measures for six data sets are shown in table 2.

TABULATION OF RESULTS OF VARIOUS PERFORMANCE MEASURES

S.No.	Measures	Data set1	Data set2	Data set3	Data set4	Data Set5	Data set6
1	Accuracy	0.95348	0.93442	0.96512	0.9553	1	0.9835
2	Sensitivity	0.9333	0.92356	0.95	0.9477	1	0.98076
3	Specificity	1	1	1	1	1	1
4	Positive Predictor Value	1	1	1	1	1	1
5	Negative Predictor Value	0.86666	0.68421	0.89655	0.7647	1	0.89655
6	False Discovery Rate	0	0	0	0	0	0
7	Mathew Correlation Coefficient	0.89938	0.79493	0.9228	0.8513	1	0.9377
8	Error	0.0465	0.06557	0.03488	0.04469	0	0.01648
9	False Prediction Rate	0	0	0	0	0	0
10	False Negative Rate	0.06666	0.0764	0.05	0.05228	0	0.01923
11	Prediction Conditioned Fallout	0	0	0	0	0	0
12	Prediction Condition Miss	0.1333	0.31578	0.103448	0.23529	0	0.103448
13	Rate of Positive Prediction	0.65116	0.792349	0.66279	0.81005	0.70454	0.840659
14	Rate Negative Prediction	0.348837	0.20765	0.3372	0.1899	0.29545	0.15934
15	Prevalance	0.69767	0.8579	0.69767	0.8547	0.70454	0.85714

Table 2 : Different performance measures

It can be observed from the result that, the proposed classifier delivers better performance i.e valuated by the performance measures evaluated in the table2. The performances of the classifier in terms of sensitivity, specificity, accuracy for six data sets are illustrated in figure 13, 14, & 15 respectively.

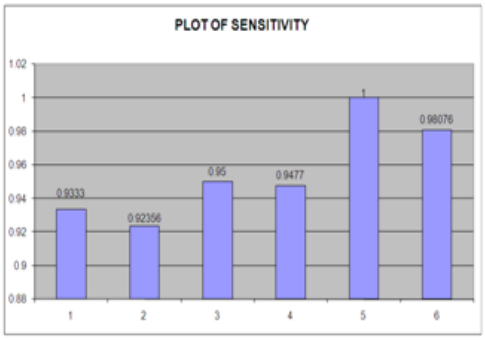

Figure 13 : Sensitivity Vs Data sets

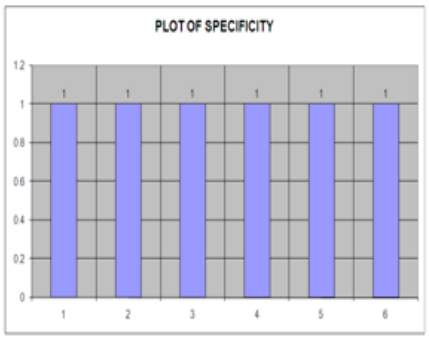

Figure 14 : Specificity Vs Data sets

It can be clearly observed from figure 13,14&15, there is a market improvement in the classification in the classification performance, once the image are fused. It can be observed from the figure 14, which is depicts the classification accuracy, the accuracy of classification for data set1 is 95.34% and accuracy of data set 3 is 96.51%. When images of data set1 & data set3 are fused and formulated dataset4, it can be clearly observed that theaccuracy is improved to 100%. This enhanced performance is clearly observed for data set 6, which has images fused data set 2 and data set 4 with different cloud covers. The classification accuracy of data set 6 stands at 98.35% while data set 2 & data set 4 is 93.53% & 95.53% respectively.

Especially with regards to data set6, the result of the classifier can be compared with the result provided in reference 5 which is of 97.9%.

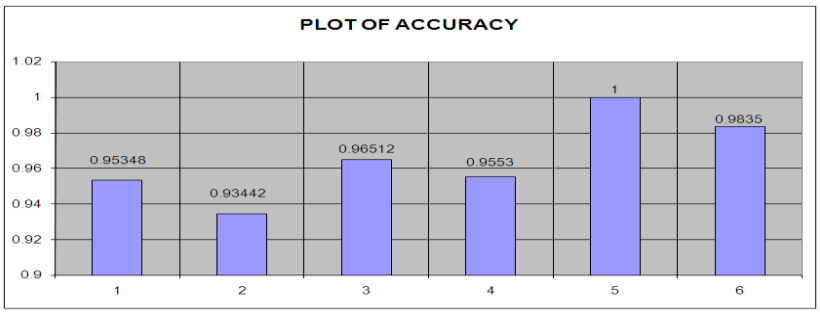

Figure 14 : Accuracy Vs Data sets

V. CONCLUSIONS

The multi spectral satellite images based volcano hotspots identification has been designed and demonstrated with following conclusions

1. An ANFIS based classifier combined with DWT & PCA feature extraction is employed for classification of satellite images.
2. The results are analysed for different classification performance for different data sets comprising multiple images having presence and absence of volcano.
3. The results validate the performance of proposed classifier in its ability to classify the presence and absence of volcano.
4. In order to improve the classification accuracy , DTCWT based image fusion has been employed sucessfully to fused images of visible and visible near infrared spectral regions.
5. It is clearly observed that, Once the images are fused using proposed approach, there is appreciable enhancement in the classification accuracy.
6. This multi spectral fused based approach can provide and improved performance especially in the images having high percentage of cloud cover. This suitability demonstrates the efficacy of the proposed approach in identification of volcano hotspots.

REFERENCES

[1]. SwetA K.Shah, and D.U. Shah. (March 2014). "Comparitive Study of Image Fusion Techniques based on Spatial and Transform domain", International Journal of Innovative Resaerch in Science, Engineering and Technology, ISSN: 2319-8753, Vol.3, Issue.3.

[2]. B. Raghavendra Reddy, and T. Ramashri. (December 2013). "Image Fusion Algorithms using different Wavelet methods and Improvement Techniques", International Journal of Advanced Research in Electrical, Electronics and Instrumentation Engineering", Vol.2, Issue 12.

[3]. Asha Das, and K. Revathy. (2007). "A Compaeative Analysis of Image Fusion Techniques for Remote Sensed Images", Proceedings of the World Congress on Engineering, Vol.I, July 2-4, London, UK.

[4]. Vaibhav R. Pandit, and R.J. Bhiwani. (June 2015). "Image Fusion in Remote Sensing Applications: A Review", Internatinal Journal of Computer Applications, (0975-8887), Vol.120, No. 10.

[5]. Tasneem Ahmed, Dharmendra Singh, Shweta, and Balasubramanian Raman. (2015). "An efficient application of fusion approach fot hot spot detection with MODIS and Palsar-1 data", Geocarto International.

[6]. Hyung-SupJung, and Sung-Whan Park,"Multi sensor Fusion of Landsat8 Thermal Infrred and Panchromatic images", Sensors, ISSN 1424-8220.

[7]. M.Masthaniah, and P. Janardhan Sai Kumar. (September 2014). "Development of Image Fusion Algorithms by Integrating PCA, Wavelet and Curvelet Transforms", International Journal of Innovative Research in Computer and Communication Engineering", Vol.2, Special issue 4.

[8]. Mohamed Ibazizen and Jacques Dauxois. (Jan.2002) "A robust principal component ananlysis", A Journal of Theoretical and Applied Statistics, ISSN:0233-1888.

[9]. Piotr Lipinski, and Mykhaylo Yatsymirskyy. (2007) "Efficient ID and 2D Dauchechies Wavelet Transformwith Application to Signal Processing", Spinger, Part II, LNCS 4432, pp.391-398.

[10]. M.Y. Gokhale, and Daljeet Kumar Khanduja. (2010) "Time Domain Signal Analysis Using Wavelet Packet Decomposition Appoach", Int. J. Communications,Networks & Sciences,3, 321-329.

[11]. Hasan Demirel, Cagri Ozcinar, and Gholamreza Anbarjafari. (April 2010). "SatelliteImage Contrast Enhancement Using Discrete Wavelet Transform andSingular Value Decomposition", IEEE Geoscience And Remote Sensing Letters, Vol. 7, No. 2.

[12]. Raafat Fahmy, Hegazy Zaher, and Abd Elfattah Kandil. (January 2015) "A Comparision between Fuzzy Inference System for Prediction", International Journal of Computer Applications, (0975-8887), Vol. 109, No. 13.

[13]. OguzGungor, and Jie Shan, "Evaluation of Satellite image fusion using Wavelet transform" Commision III, WG III/6.

[14]. Shutao Li. (2008) "Multisensor Remote Sensing Image Fusion Using Stationary Wavelet Transform: Effects of Basis And Decomposition Level", International Journal of Wavelets, Multiresolutionand Information Processing, Vol. 6, No. 1 37–50.

[15]. Alessandro Piscini, and Valerio Lombardo. (2014). "Volcanic hot spot detection from optican multispectral remote sensing data using artificial neuaral networks" Geophysical Journal International, 196,1525-1535.

[16]. Mary Sincy, and M. Mathurakani.(Jan-Feb 2015). "A Novel Image Fusion Technique using Dual Tree Complex Wavelet Transform", International Journal of Engineering Research and General Sciences, ISSN No. 2091-2730 Vol.3, Issue1.

[17]. RudraPratap Singh, RajivaDwivedi, and Sandeep Negi. (September 2012) "Comparative Evaluation of DWT and DT-CWT for Image Fusion and De-noising", International Journal of Applied Information Systems (IJAIS) – ISSN : 2249-0868, Volume 4– No.2.

[18]. SouparnikaJadhav.(July 2014). "Image Fusion Based On Wavelet Transform", International Journal of Engineering Research, ISSN:2319-6890, Vol. No.3, Issue No.7, pp : 442-445.

[19]. Rohit Raj Singh, and M. Ravi Mishra. (April 2015). " Benefits of Dual Tree Complex Wavelet Transform over Discrete Wavelet Transform for image fusion", International Journal for Innovative Research in Science & Technology, Vol.1, Issue 11, ISSN : 2349-6010.

[20]. Dineshkumar, and DVS Nagendrakumar. (Sep-2015)" Image De-Noising Using Dual-Tree Complex Wavelet Transform for Satellite Applications", International Research Journal of Engineering and Technology, e-ISSN: 2395-0056, Vol. 02, Issue 06.

[21]. Yong Yang, Song Tong, Shuying Huang, and Pan Lin. (2014) "Dual-Tree Complex Wavelet Transform and Image Block Residual-Based Multi- Focus Image Fusion in Visual Sensor Networks", Sensors, 14, 22408-22430; DOI:10.3390/s141222408.

[22]. A. M. El Ejaily, F. Eltohamy, M. S. Hamid, and G. Ismail. (January 2011,) "An Image Fusion Method Using DT-CWTand Average Gradient", International Journal of Computer Science and Mobile Computing, ISSN 2320–088X IJCSMC, Vol. 3, Issue. 1, pg.272 – 280.

[23]. http://ava.jpl.nasa.gov